Isothermal and Nonisothermal Crystallization Kinetics of MC Nylon and Polyazomethine/MC Nylon Composites

Xiongwei Qu,[1] Huili Ding,[2] Jianying Lu,[1] Yuexin Wang,[1] Liucheng Zhang[1]

[1]*Institute of Polymer Science and Engineering, School of Chemical Engineering, Hebei University of Technology, Tianjin, 300130, People's Republic of China*
[2]*College of Materials Science and Engineering, Tianjin University, Tianjin, 300072, People's Republic of China*

ABSTRACT: Crystallization kinetics of MC nylon (PA6) and polyazomethine (PAM)/MC nylon (PAM/PA6) both have been isothermally and nonisothermally investigated by different scanning calorimetry (DSC). Two stages of crystallization are observed, including primary crystallization and secondary crystallization. The Avrami equation and Mo's modified method can describe the primary stage of isothermal and nonisothermal crystallization of PA6 and PAM/PA6 composite, respectively. In the isothermal crystallization process, the values of the Avrami exponent are obtained, which range from 1.70 to 3.28, indicating an average contribution of simultaneous occurrence of various types of nucleation and growth of crystallization. The equilibrium melting point of PA6 is enhanced with the addition of a small amount of rigid rod polymer chains (PAM). In the nonisothermal crystallization process, we obtain a conve-

nient method to analyze the nonisothermal crystallization kinetics of PA6 and PAM/PA6 composites by using Mo's method combined with the Avrami and Ozawa equations. In the meanwhile, the activation energies are determined to be −306.62 and −414.81 KJ/mol for PA6 and PAM/PA6 (5 wt %) composite in nonisothermal crystallization process from the Kissinger method. Analyzing the crystallization half-time of isothermal and nonisothermal conditions, the over rate of crystallization is increased significantly in samples with a small content of PAM, which seems to result from the increased nucleation density due to the presence of PAM rigid rod chain polymer. © 2004 Wiley Periodicals, Inc. J Appl Polym Sci 93: 2844–2855, 2004

Key words: differential scanning calorimetry (DSC); nylon; crystallization; activation energy

INTRODUCTION

Monomer Casting Nylon (MC nylon, referred to as PA6) has found wide application in many fields of bearing utilization, especially in the lightly loaded bearing with poor or no lubrication, but water absorption, thermal expansion, and low load ability have limited its use in wet and high load conditions. Various techniques have been used to modify its properties, such as polyblends and filled and reinforced composites.[1–4]

Recently, Morgan and coworkers[5,6] reported the preparation of a variety of wholly aromatic melt anisotropic polyazomethines (PAMs) and their fibers. These

synthetic reactions of dialdehyde with diamine were quick, efficient, and had several advantages,[7,8] and these polymers showed good mechanical properties at very high temperatures, resulting from the incorporation of nitrogen atoms into the conjugated molecular chains and potential usage in engineering applications. For example, a small amount of added PAM could be used as a reinforcing rigid rod polymer in polyamides.[9] Such reinforced systems displayed enhanced tensile strength, modulus, and thermal stability over conventional short-fiber–reinforced composites.

Although PAM/PA6 composites can be prepared via a solution blending of components, phase separation may occur during melt processing. A possible solution to this problem is to synthesize PAM, a rigid rod polymer, in ε-caprolactam monomers, which can be later polymerized as a matrix.[5,9] Such polymerization is called *in situ* polymerization. These composites can not only uniformly disperse in matrix, but might also obtain improved mechanical properties without phase separation. In the previous work, the structure and morphology of PAM/PA6 composites were investigated by FTIR, UV spectra, wide-angle X-ray diffraction (WAXD), differential scanning calorimetry (DSC), thermogravimetric analysis (TGA), etc.[10] The

crystallization of PA6 is often influenced not only by processing conditions, but also by the presence of the reinforcing phase (PAM), which generally favors heterogeneous nucleation by acting as nucleation sites for crystallization.[11,12] As PA6 is a semicrystalline polymer and its mechanical and thermal properties are strongly dependent on the processing conditions, analysis of the isothermal and nonisothermal crystallization kinetics of PA6 and PAM/PA6 composites is carried by DSC in this article.

EXPERIMENTAL

Materials and preparation

Terephthalaldehyde (TPA) (Tianjin Chem. Co., China) is purified by recrystallization with deioned water. 4,4′-Diaminediphenyl ether (4,4′-DAPE), sodium hydroxide, and isocyanate (Tianjin Chem. Co., China), analytical reagent quality, are used as supplied. ε-Caprolactam (Sijiazhuang Chemical Fiber Co., China) is dried under vacuum at 80°C for 4 h before use. PAM rigid rod chain polymer is the product of a polycondensation reaction of TPA with 4,4′-DAPE. The samples of PAM/PA6 composite are prepared through *in situ* polymerization in our laboratory.

ε-Caprolactam (50 g) is placed into a three-necked 500-mL round-bottom flask, equipped with stirrer, thermometer, and gas inlet and outlet. The caprolactam is heated to a complete melt while a slow stream of dry nitrogen is passed through the apparatus. Terephthalaldehyde (6.6 g) is added and dissolved into the melt. Separately, a solution of 9.85 g 4,4′-DAPE is prepared in 50 g of molten ε-caprolactam in a three-necked 250-mL round-bottom flask. This solution is poured into the TPA/ε-caprolactam melt with vigorous agitation. The solution instantly turns a deep red color, indicating a reaction of the TPA and 4,4′-DAPE has occurred. The latter flask is rinsed out with about 30 mL of toluene into the TPA solution. After about 5 min at a temperature of 80°C, a turbid orange–red liquid results, having the appearance and the viscosity of a thin paint. The reaction solution is continuously heated to about 160°C and maintained for 30 min. The product is distilled to remove the toluene and the water produced by reaction of the TPA and 4,4′-DAPE under vacuum, and high molecular weight PAM is obtained in the solution. Next, sodium hydroxide (initiator) is dispersed into the solution and maintained until the sodium hydroxide is dispersed finely to remove the by-product that formed under vacuum. The solution then is continuously cooled down to 140°C under stirred conditions and filled in nitrogen. Isocyanate (coinitiator) is added, and dispersed in solution for a period of 5 min to get a yellow-colored solution. After that, the solution is quickly poured into a plated mode, which is placed in an oven with a temperature of 170°C. Kept for 2 h to react completely, the final product, PAM/PA6 composite, is prepared.

The ratios of PAM/PA6 are 0/100, 2.5/97.5, 5/95, and 7.5/92.5 by weight, each referring to 0, 2.5, 5, and 7.5% for PAM contents. PAM/PA6 composites are dried in a vacuum oven at 80°C for 24 h before use.

Differential scanning calorimetry

Isothermal and nonisothermal crystallization kinetics are carried out using a Dupont 2000 DSC2910 differential scanning calorimeter equipped with a DPC data station. All DSC measurements are performed under dry nitrogen flow ($\sim$ 8 mg) and an empty aluminum pan is used as reference.

Isothermal and nonisothermal crystallization process

The samples are heated quickly (at 80°C/min) to 250°C, the temperature remaining unchanged for 10 min to ensure total relaxation of the samples and to eliminate the influence of thermal history. They then are rapidly cooled to the designated crystallization temperatures (T_c), which contain five different temperatures ranging from 191 to 203°C for the isothermal crystallization process (Fig. 1) and four different cooling rates at 1, 2, 5, and 10°C/min, respectively, to 150°C for the nonisothermal crystallization process (see Fig. 6). The exothermic curves of heat flow as a function of time are recorded and investigated.

RESULTS AND DISCUSSION

Isothermal crystallization kinetic analysis

Isothermal crystallization kinetics from the avrami equation

Isothermal crystallization is studied by cooling the melt rapidly to crystallization temperature, T_c. Since the Avrami equation has been widely used to analyze isothermal crystallization,[13,14] it is assumed that the relative degree of crystallinity, X_t, which develops at time t, is

$$X_t = \frac{X_c(t)}{X_c(t = \infty)} = \frac{\int_0^t \frac{dH(t)}{dt}\,dt}{\int_0^\infty \frac{dH(t)}{dt}\,dt} \tag{1}$$

$$1 - X_t = \exp(-Kt^n) \tag{2}$$
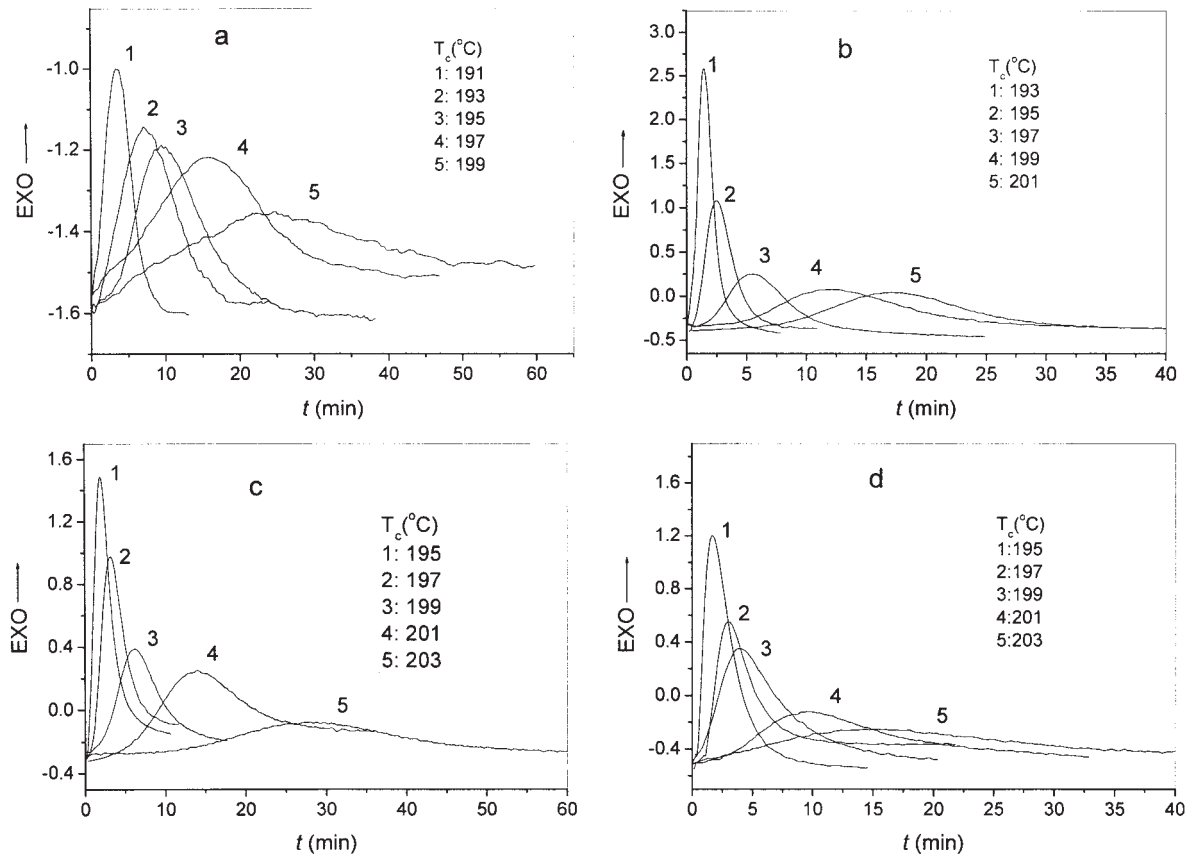
$$\lg[-\ln(1 - X_t)] = \lg K + n \lg t \tag{3}$$

Figure 1 DSC curves during isothermal crystallization of PAM/PA6 composites at different crystallization temperatures with various PAM contents (a) 0%, (b) 2.5%, (c) 5%, (d) 7.5% in weight percent.

where $X_c(t)$ and $X_c(t = \infty)$ are the fractional extent of crystallinity at time t and at the end of the primary process, respectively; dH/dt is the rate of crystallization heat evolution at time t. The parameter K is a composite rate constant involving both nucleation and growth rate parameters under isothermal conditions. The Avrami exponent, n, is a mechanism constant, which depends on the type of nucleation and growth rate parameters.

The crystallization half-time $t_{1/2}$ is defined as the time at which the extent of crystallization is 50% complete and can be determined from eq. (4). That is

$$t_{1/2} = (\ln 2/K)^{1/n} \qquad (4)$$

Figure 1 records the diagrams of heat flow as a function of time for PAM/PA6 composites. Figures 2 and 3 plot X_t versus lg$t$ and the double logarithmic plot of lg$[-\ln(1 - X_t)]$ versus lg$t$ at the different crystallization temperatures. It can be seen from Figure 2 that the relative crystallinity is a strong function of crystallization temperature (T_c). Each curve shows an initial linear portion during most of crystallization time and then departs the linear relationship. A slow increase of crystallinity with time after most of the crystallization

is observed indicates the existence of a secondary crystallization of PA6 and PAM/PA6 composites caused by the spherulite impingement and perfection of internal spherulite crystallization in the later stage of isothermal crystallization process. Therefore, the Avrami eq. (1) can describe well the isothermal crystallization kinetics for PA6 and PAM/PA6 composites in the primary stage. Table I lists the fitted crystallization kinetics parameters from the slope and intercept of the Avrami plot (Fig. 3), n, K, and the half-life of crystallization ($t_{1/2}$). It is indicated that K values of PA6 and PAM/PA6 composites increase distinctly with the decrease in crystallization temperature (T_c) and those of $t_{1/2}$ decrease rapidly. The values of the Avrami exponent are obtained, which range from 1.70 to 3.28, indicating an average contribution of simultaneous occurrence of various types of nucleation and growth of crystallization. The crystallization mode of PA6 might be the mixture with one-dimensional, needle-like and two-dimensional, circular, diffusion-controlled growth with thermal nucleation. There is a noticeable difference in the n value with crystallization temperature. At lower crystallization temperatures, their exponents are similar between the integers 2 and 3. However, at higher crystallization temperatures, the
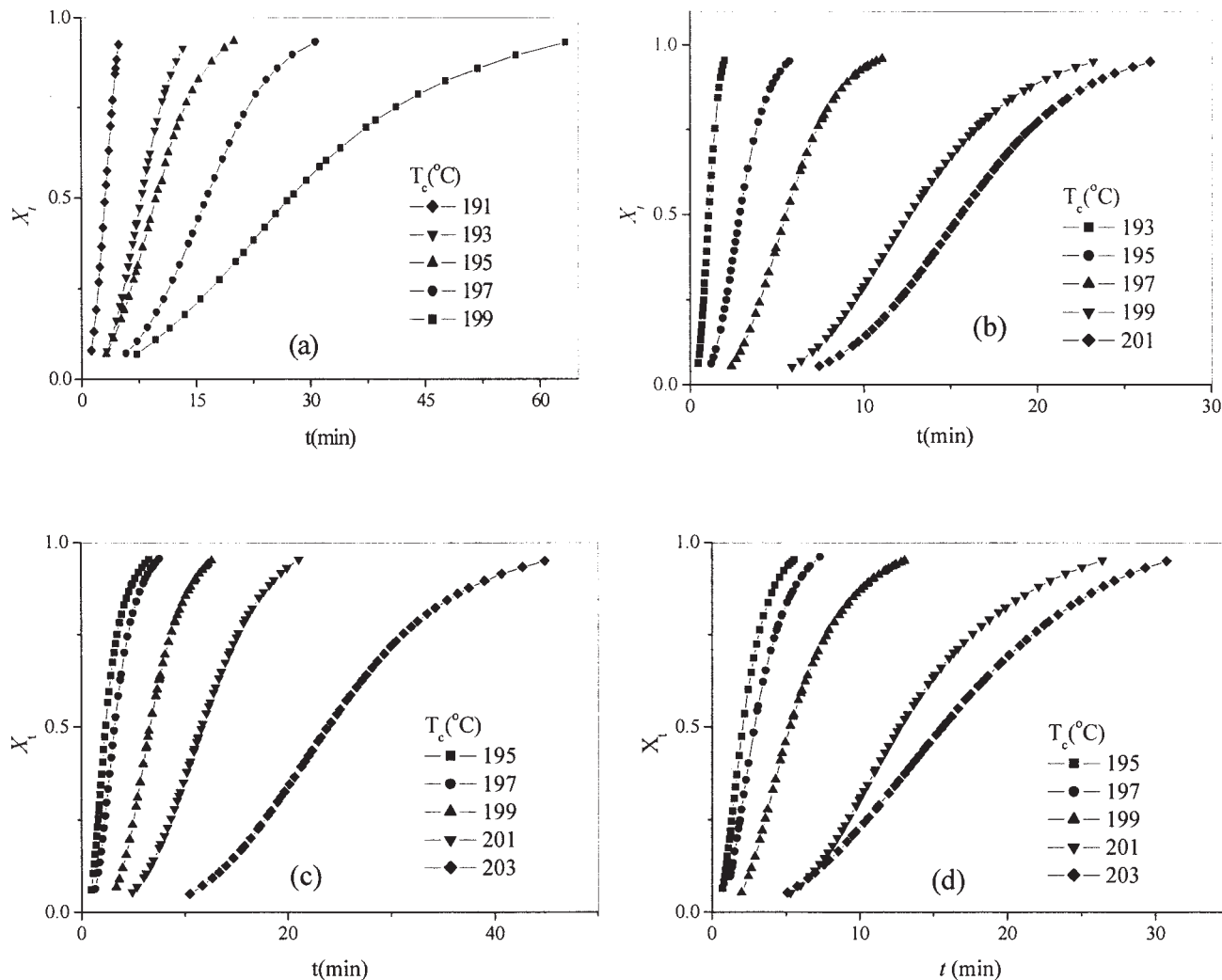
Figure 2 Plots of the relative crystallinity versus time for PAM/PA6 composites with different PAM contents (a) 0%, (b) 2.5%, (c) 5%, (d) 7.5% in weight percent.

exponent of PA6 decreases to 1.70, while those of PAM/PA6 composites reach 3.2. The above results imply that PA6 and PAM/PA6 composites have the same nucleation and growth mechanism only at lower temperatures. As the temperature increases, the crystallization rates of the PAM/PA6 composites become faster than those for the corresponding PA6 polymer.

With the crystallization temperature increase, the crystallization exotherms shift to higher temperatures and become flat (Fig. 1); it implies that the total crystallization time is lengthened and the crystallization rate decreases with the increased T_c (Table I).

From the data listed in Table I, it can be seen that the values of $t_{1/2}$ of PAM/PA6 composites are lower than those of PA6 and decrease with the increase of PAM content, as shown in Figure 4. At higher temperatures, such as 199°C, the crystallization rates for all the composites are higher than those of the pure PA6. Reported in previous paper, the crystal morphologies of PA6 and PAM/PA6 composites are spherulite crystal-line structures showing dark Maltese crosses.[10] PA6 contains relatively large crystals, whereas a dense granular texture of crystals is formed in the presence of PAM rigid rod polymer and the size of spherulite becomes smaller too. This indicates that the presence of rigid rod PAM chains may play a role of increasing the nucleation sites and that the increased nucleation sites lead to an increase in the overall rate of crystallization.

The equilibrium melting point

Before carrying on quantitative analysis of crystallization behavior, the equilibrium melting point temperature must be determined as accurately as possible, since the thermodynamic parameters derived from the experimental K_g are very sensitive to its values. Therefore, a careful DSC study should be performed to estimate the equilibrium melting point for polymers.
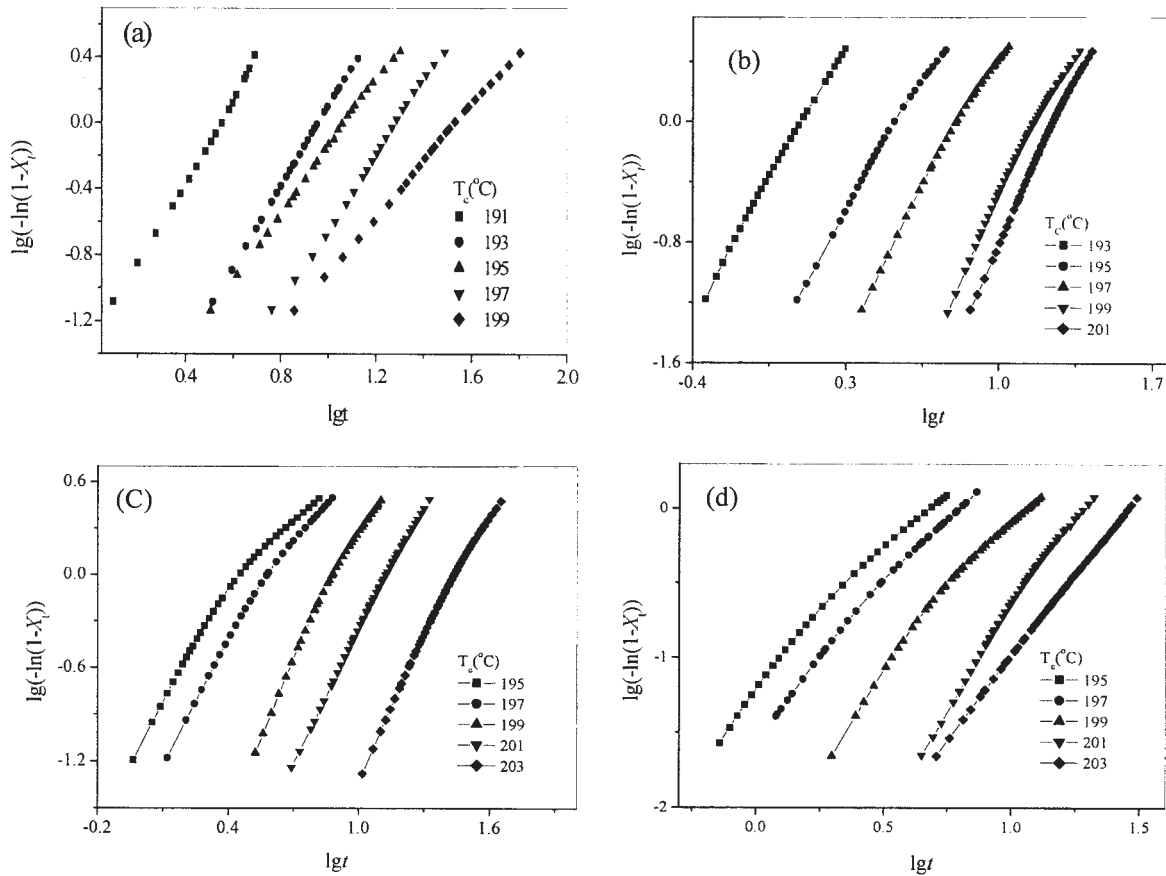
Figure 3 Plots of $\lg[-\ln(1 - X_t)]$ versus $\lg t$ for isothermal crystallization for PAM/PA6 composites at indicated temperatures (a) 0%, (b) 2.5%, (c) 5%, (d) 7.5% in weight percent.

TABLE I
Kinetics Data for Isothermal Crystallization of PAM/PA6 Composites *In Situ* Polymerization

PAM content (wt %)	$T_c(^{\circ}C)$	n	I gK	K	$t_{1/2}$(min)
0	191	2.50	−1.3645	0.04320	3.03
	193	2.45	−2.3453	0.004515	7.80
	195	2.36	−2.6735	0.002121	11.62
	197	1.71	−2.4336	0.003685	21.38
	199	1.70	−2.6073	0.002470	27.55
	193	2.57	−0.8755	0.1332	1.90
	195	2.65	−1.3771	0.04196	2.88
2.5	197	2.90	−2.30815	0.004919	5.51
	199	3.20	−3.6811	0.000208	12.60
	201	3.28	−4.0886	8.15E-05	15.74
	195	2.49	−1.0671	0.08568	2.31
	197	2.57	−1.4590	0.03475	3.21
5	199	3.20	−2.7937	0.001608	6.68
	201	2.80	−3.1679	0.000679	11.87
	203	2.94	−4.21996	6.03E-05	24.17
	195	2.13	−0.82032	0.1512	2.04
	197	2.12	−1.1370	0.07294	2.89
7.5	199	2.44	−1.9234	0.01193	5.27
	201	2.85	−3.3046	0.000496	12.68
	203	2.19	−2.7804	0.001658	15.71

Heretofore, as a main approach, the Hoffman–Weeks equation has been widely used to estimate the equilibrium melting point of polymers.

According to theoretical consideration by Hoffman and Weeks,[15] the equilibrium melting point of polymers can be obtained solely from DSC measurements by plotting the observed apparent melting temperature T_m versus the crystallization temperature T_c. PA6 is isothermally melt crystallized at different crystallization temperatures. The samples are then melted at the heating rate of 10°C/min. The equilibrium melting point temperature is obtained by the intersection of the resulting straight line with the line $T_m = T_c$. Assuming chain folding during crystallization, the dependence of the apparent melting temperature T_m on the crystallization temperature T_c is given by

$$T_m = T_m^0 \left(1 - \frac{1}{2\beta}\right) + \frac{1}{2\beta} T_c \tag{5}$$

where T_m^0 is the equilibrium melting point and β is the lamellar thickening factor, which describes the growth of lamellar thickness during crystallization. Under equilibrium conditions, β is equal to 1.[16] At the higher
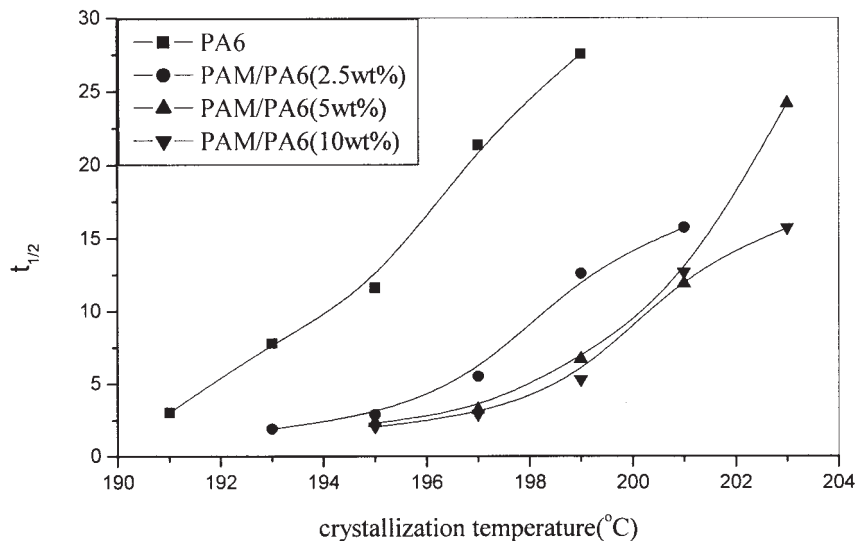
Figure 4 Half-time of crystallization, $t_{1/2}$, in the isothermal crystallization processes at different temperatures for the specimens of PA6 and PAM/PA6 composites.

crystallization temperatures, the slope of the plots is 0.5 and extrapolates to a thermodynamic melting point temperature of $T_m^0 = 223.6°C$ for PA6 (Fig. 5).

Using a similar method, we could obtain the equilibrium melting points for PAM/PA6 composites. Table II lists the values of T_m^0 of PA6 with different contents of PAM rigid rod polymer. The equilibrium melting points increase with the increase in PAM content. We have purposed that the effect of T_m^0 increase may result from some hindrance in the melting process of PA6 caused by the presence of PAM. The action between PAM and PA6 gives the PAM/PA6 composite a suitable compatibility by forming a hydrogenated bond. The PAM chains rejected previously in the amorphous phase during crystallization of PA6 delays the starting mobility of polymer segments in the regions of lamellae surfaces during the polymer melting process. Thus, the PA6 sample has a more rigid amorphous phase containing more PAM, and it melts at a higher temperature.

Nucleation rate parameter k_g

In 1949, Turnbull and Fisher[17] put forward the Turnbull–Fisher expression to describe the crystallization
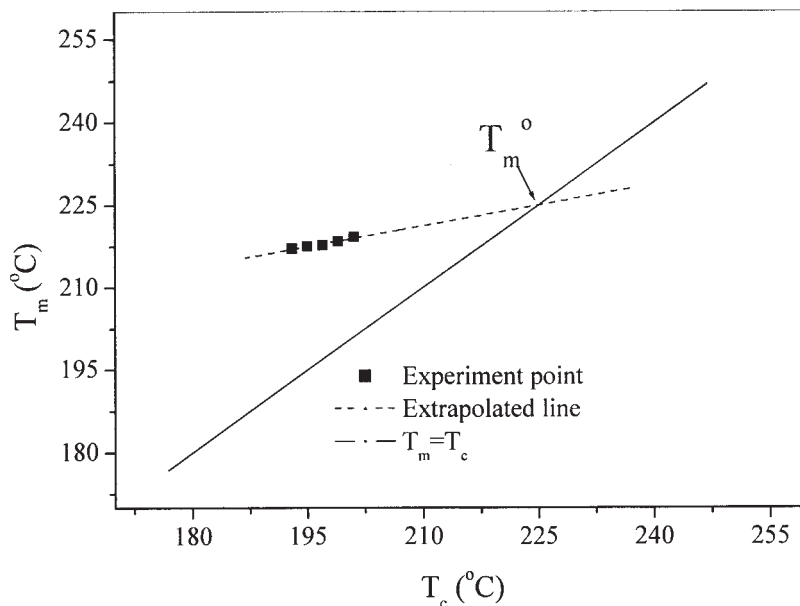

Figure 5 The determination of the equilibrium melting point for PA6 in the isothermal crystallization process.

TABLE II
Equilibrium Melting Point of PA6 with Different
Content of PAM

PAM content (wt %)	0	2.5	5	7.5
T_m^0 (°C)	223.6	225.2	226.4	230.8

TABLE III
Values of K_g for PA6 and PAM/PA6 Composites with
Different PAM Contents

PAM content (wt %)	0	2.5	5	7.5
K_g ($\times 10^5 K^2$)	7.21	6.67	6.30	5.92

process. To make the Turnbull–Fisher expression suitable for the crystallization process in large supercooling rates, Hoffman et al.[18] analyzed the nucleation growth rate, G, and obtained the famous Lauritzen–Hoffman equation, as follows:

$$G = G_0 \exp\left[-\frac{U^*}{R(T_c - T_\infty)}\right]\exp\left(-\frac{K_g}{T_c \times \Delta T \times f}\right) \quad (6)$$

where G is the nucleation rate forming a critical spherulitic size, G_0 is the preexponential factor, U^* is the transport activation energy, R is the gas constant, T_c is the crystallization temperature, T_∞ is a hypothetical temperature below which all viscous flow ceases, K_g is a nucleation parameter, ΔT is the degree of supercooling ($\Delta T = T_m^0 - T_c$), T_m^0 is the equilibrium melting point, and f is a correction factor to account for the variation in the bulk enthalpy of fusion with the temperature.

According to Hoffman et al.,[18] the U^* and T_∞ may be assigned as universal values of 1,500 cal/mol and T_g –30 K, respectively, T_g being the glass transition temperature. In this study, the glass transition temperature of PA6 is taken as 50°C,[19] and f is close to unity used here to calculate. We rearrange eq. (6) as

$$\lg G + \frac{U^*}{2.303R(T_c - T_\infty)} = \lg G_0 - \frac{K_g}{2.303 T_c \Delta T f} \quad (7)$$

A plot of $\lg G + U^*/2.303R(T_c - T_\infty)$ versus $1/T_c \Delta T f$ is shown in Figure 6, exhibiting a linear relation for all PAM contents. Hence, the values of the slope, K_g, for PAM/PA6 composites can be obtained and is listed in Table III.

From the results seen in Table III, the values of K_g are lowered with the increase of PAM content. As discussed above, PAM chains provide heterogeneous nucleation sites and thus enhanced the overall rate of PA6 crystallization in isothermal experiments. This result of the Lauritzen–Hoffman equation agrees well with that of the Avrami equation.

Nonisothermal crystallization kinetics analysis

Avrami equation by Jeziorny modified

We have discussed isothermal crystallization kinetics for PAM/PA6 composites. In practice, production and processing of the polymer are often carried out under nonisothermal conditions. Therefore, the investigation of the kinetics of polymer crystallization under
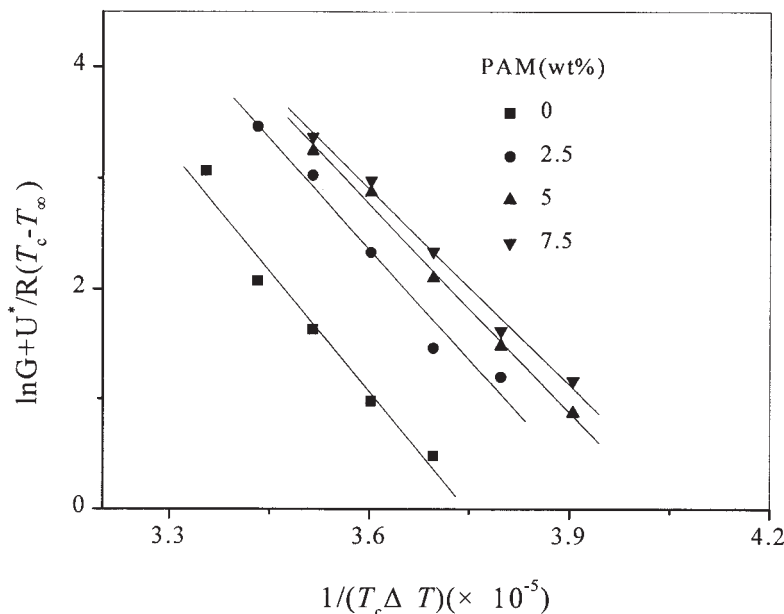

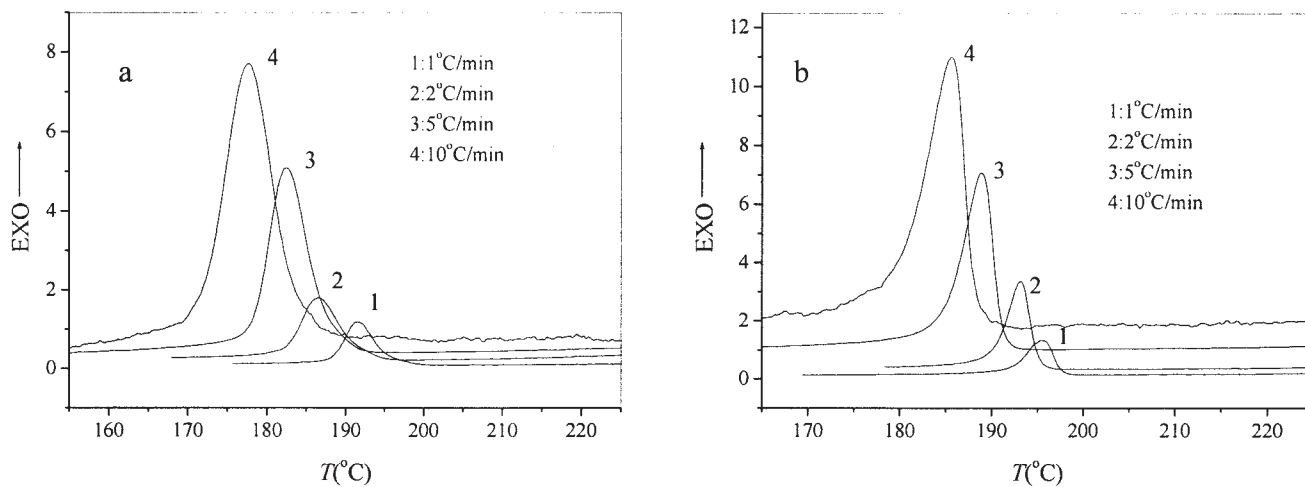**Figure 6** Lauritzen—Hoffman plots for PAM/PA6 composite systems.

Figure 7 DSC curves during nonisothermal crystallization for (a) PA6 and (b) PAM/PA6 (5 wt %) composite at different cooling rates.
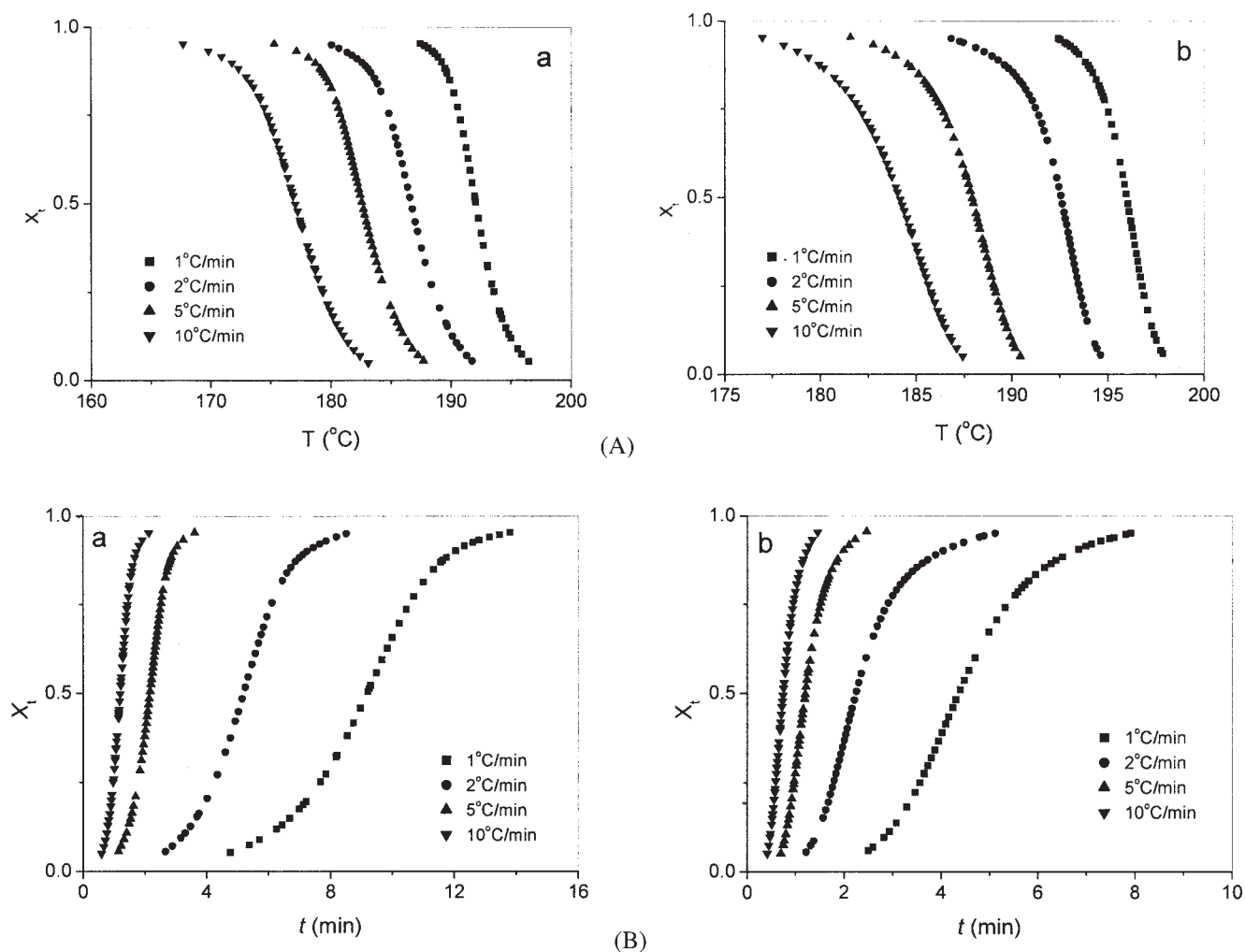

Figure 8 The relative crystallinity X_t: (A) at different crystallization temperatures, T, and (B) at different crystallization times, t, in the process of nonisothermal crystallization for (a) PA6 and (b) PAM/PA6 (5 wt %) composite.
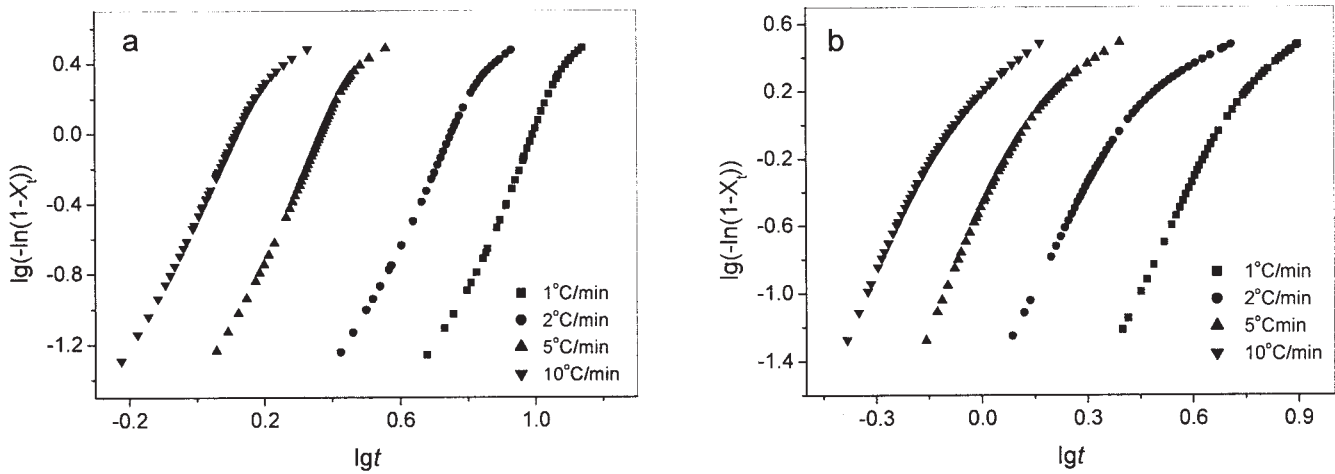
Figure 9 Plots of lg[−ln(1 − X_t)] versus lg$t$ during the nonisothermal crystallization process for (a) PA6 and (b) PAM/PA6 (5 wt %) composite at indicated cooling rate.

nonisothermal conditions is of great significance for the technological optimization and manufacture of high-performance polymeric materials. In the following, nonisothermal crystallization kinetics will be discussed. Figures 7(a) and 7(b) show the crystallization exotherms of PA6 and PAM/PA6 composite (5 wt % PAM content) at various cooling rates, Φ, respectively. T_p is the peak temperature at which the crystallization rate reaches the maximum, and it shifts to a low temperature region as the cooling rate increases. There is much time for PA6 to nucleate and grow at high temperatures under low cooling rate conditions. Therefore, this crystallization is controlled by a nucleation process. Meanwhile, the value of T_p for 5 wt % PAM/PA6 composite is higher than that of pure PA6.

From the DSC digital information, we calculate the values of the weight fraction crystallinity, X_t, at different crystallization temperatures, T, shown in Figure 8(A). We obtain a series of reversed S-shaped curves. During the nonisothermal crystallization process, the relationship between crystallization temperature T and time t is given by

$$t = |T_0 - T|/\Phi \tag{8}$$

T_0 is the initial temperature (250°C) when crystallization begins ($t = 0$). T is the temperature at time t. The values of the T axis in Figure 8(A) could be transformed into crystallization time t [shown in Fig. 8(B)]. Because of the spherulitic impingement in the later crystallization stage, the curves become S-shaped. We can obtain the values of T or t at the various cooling rates from Figure 8 at a random relative crystallinity X_t.

Jeziorny considered that the primary stage of nonisothermal crystallization could be described by

the Avrami equation at a constant cooling rate.[20] He obtained the following equation:

$$1 - X_t = \exp(-Z_t t^n) \tag{9}$$

where Z_t is the primary composite rate constant in the nonisothermal crystallization process, and it should be corrected by the cooling rate $\Phi = dT/dt$. The final form of the rate parameter characterizing the kinetics of nonisothermal crystallization is given as follows:

$$\lg Z_c = \frac{\lg Z_t}{\Phi} \tag{10}$$

Drawing the straight line corresponding to lg[−ln(1 − X_t)] versus lg$t$ by using eq. (9), we can determine the value of the Avrami exponent n and the rate parameter Z_t from the slope and the intercept (Fig. 9). The values of n, Z_t, and $t_{1/2}$ are shown in Table IV. Like the process of isothermal crystallization (Fig. 3), all curves are divided into the following two sections: the primary crystallization stage and the secondary crystallization stage. At the secondary stage, the straight line tends to depart at 60% relative crystallinity for PAM/PA6 composite and at 80% relative crystallinity for PA6. The result also indicates the existence of a secondary crystallization in the process of nonisothermal crystallization for PA6 and PAM/PA6 composite. Therefore, the Avrami equation can be used to treat the nonisothermal crystallization process. At the primary stage, the Avrami exponent, $n_1 > 4$, indicates that the mode of the nucleation and growth at the primary stage of the nonisothermal crystallization for PA6 and PAM/PA6 composite is more complicated than that of the isothermal crystallization process. The crystallization rate $t_{1/2}$ decreases with the increase of

TABLE IV
Parameters of Nonisothermal Crystallization Kinetics for PA6 and PAM/PA6 (5 wt %) Composite

Sample	Φ (°C/min)	Primary stage		Secondary stage		$t_{1/2}$ (min)
		n_1	Z_{t1}	n_2	Z_{t2}	
PA 6	1	4.71	2.04×10^{-5}	1.93	0.01941	9.16
	2	4.27	6.15×10^{-4}	1.67	0.08381	5.19
	5	4.41	0.02334	1.37	0.5291	2.16
	10	4.04	0.3275	1.42	1.047	1.20
PAM/PA6 (5wt%)	1	4.39	1.08×10^{-4}	1.64	0.1004	4.36
	2	4.07	0.02624	1.21	0.4224	2.23
	5	4.52	0.3119	1.58	0.7630	1.19
	10	4.25	2.5582	1.74	1.599	0.74

the cooling rate Φ for PA6 and PAM/PA6 composite. Increasing the supercooling rate could provide the system with more energy to quicken the activity of chain segment, thus resulting in increasing the crystallization rate parameter, Z_c. Meanwhile, $t_{1/2}$ for PA6 is larger than that of PAM/PA6 composite, and it indicates that the presence of PAM rigid rod polymer initiates the nucleation in PA6 crystallization process and that the increased nucleation sites lead to an increase in the overall rate of crystallization as in the isothermal crystallization process. At low cooling rates, crystallites may have enough time to develop into the principal lamellae of spherulite, and thus the size of crystallites becomes larger.

From Table IV, it can be seen that the average values of the Avrami exponent, n_2, are about 1.6, suggesting that the mixture mode of one-dimensional and needle-like crystal growth occurs in the secondary stage of the crystallization. In the meantime, the crystallization rate, $t_{1/2}^{-1}$ increases with the increase of the cooling rate, Φ, showing nucleation control of crystallization.

Ozawa equation in nonisothermal crystallization kinetics

Considering the effect of Φ, Ozawa shifted eq. (8) to the Avrami eq. (9) and got the following for nonisothermal crystallization at T crystallization temperature:[21]

$$1 - X_t = \exp[-K(T)/\Phi^m] \qquad (11)$$

$$\lg[-\ln(1 - X_t)] = \lg K(T) - m \lg \Phi \qquad (12)$$

where m is the Ozawa exponent, and $K(T)$ is the kinetics crystallization rate constant. Drawing the plot of $\lg[-\ln(1 - X_t)]$ versus $\lg\Phi$ according to eq. (12), we should obtain a series of straight lines, but we do not obtain straight lines in Figure 10. From Figure 10, it is evident that the Ozawa analysis does not adequately describe the nonisothermal crystallization kinetics because a large portion of the crystallization is attributed to the secondary process. Ozawa assumed that the effects of secondary crystallization were negligible because it occurred in the later period and the tempera-
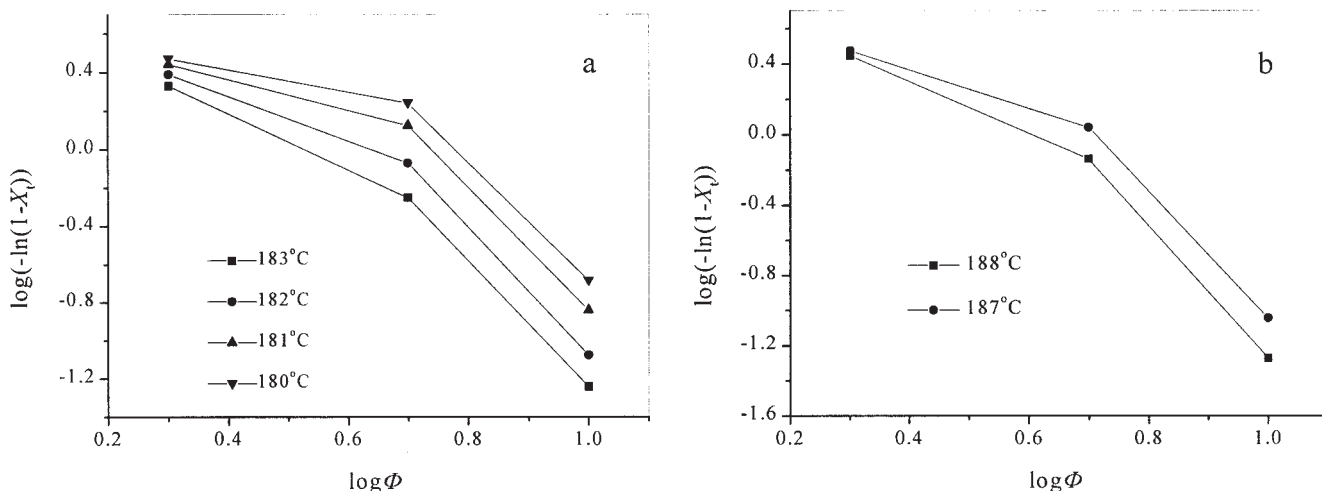

Figure 10 The plot of $\lg[-\ln(1 - X_t)]$ versus $\lg \Phi$ from the Ozawa equation for (a) PA6 and (b) PAM/PA6 (5 wt %) composite.
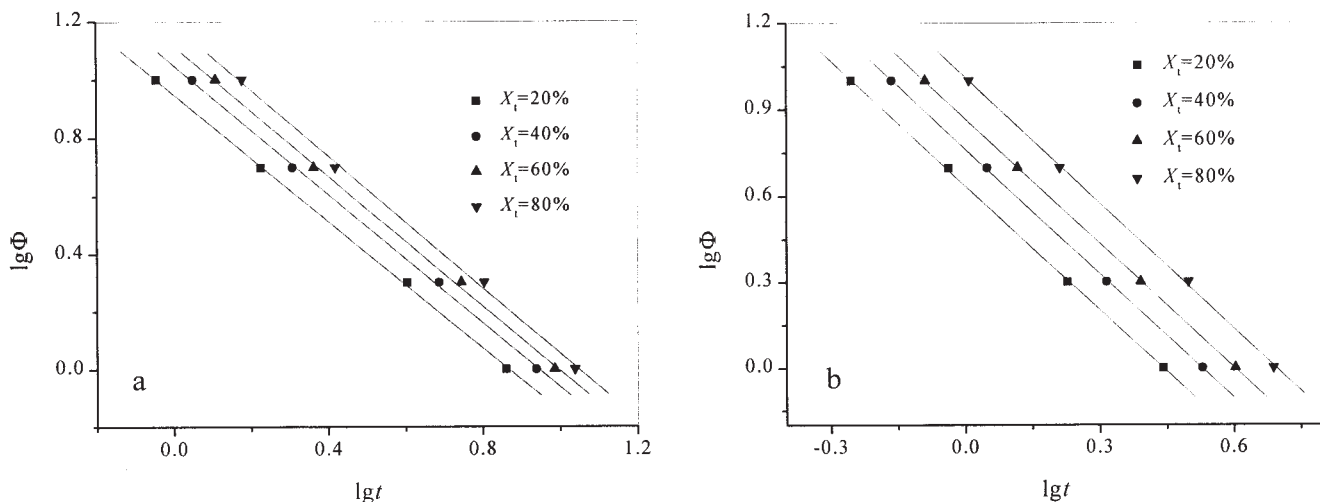
Figure 11 The plot of lg Φ versus lg t from the combined Avrami and Ozawa equation for (a) PA6 and (b) PAM/PA6 (5 wt %) composite.

ture decreased in the cooling crystallization process. Although it takes place in the later stage, the secondary crystallization is influenced greatly by the outside factors such as the cooling rate, and the effect could not be neglected for the nonisothermal crystallization of some polymer systems.

Another reason for the failure of the Ozawa model may be due to the quasiisothermal nature of the treatment. Failure of the model may be attributed to the fact that the experimental data are obtained from widely varying physical states of the system.

Mo's method of combining the Avrami equation and the Ozawa equation

To find a method to describe exactly the nonisothermal crystallization process, Mo[22,23] obtained the following by associating eqs. (9) and (11):

$$\lg Z_t + n \lg t = \lg K(T) - m \lg \Phi \qquad (13)$$

$$\lg \Phi = \frac{1}{m} \lg \frac{K(T)}{Z_t} - \frac{n}{m} \lg t \qquad (14)$$

let $F(T) = [K(T)/Z_t]^{1/m}$, and $a = n/m$. n is the Avrami parameter, and m is the Ozawa exponent. $F(T)$ means the value of the cooling rate, which has to be chosen at unit crystallization time when the measured system amounts to a certain degree of crystallization. $F(T)$ has a definite physical and practical meaning. By means of front assumptions, he obtained

$$\lg \Phi = \lg F(T) - a \lg t \qquad (15)$$

At a certain degree of crystallization of PA6 and PAM/PA6 composite, drawing the plot of lgΦ versus

lg$t$ according to eq. (15) is shown in Figure 11. When the cooling rate is very small ($\Phi = 1°C/min$), the crystallization time t is extended and causes the spherulite impingement and perfection of the internal spherulite in the later stage. Using a straight line to fit these data points, one can obtain a series of lines with slope $= -a$ and intercept $= \lg F(T)$, listed in Table V. The values of $F(T)$ increase with an increase of crystallinity and the values of a are constant approximately. Meanwhile the cooling rate Φ for PAM/PA6 composite is slower than that of PA6, which indicates that the crystallization rate of PAM/PA6 composite is faster than that of pure PA6.

Crystallization activation energy ΔE

Considering the influence of the various cooling rates Φ in the nonisothermal crystallization process, Kissinger thought the activation energy ΔE could be determined as follows:[24]

TABLE V
Values of $F(T)$, a, and ΔE for Nonisothermal Crystallization of PAM/PA6(5 wt %) Composite

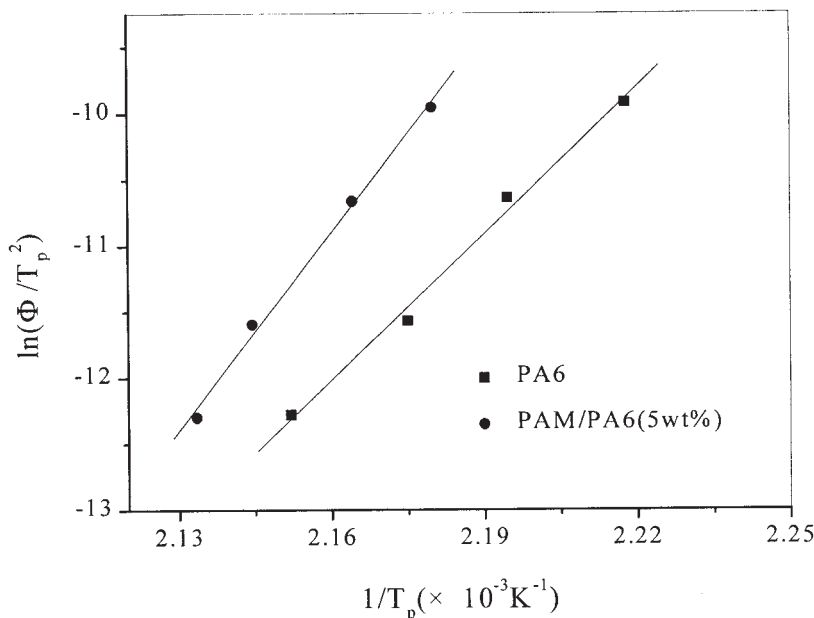| PAM content (wt %)	X_t (%)	lg$F(T)$	$F(T)$	a	ΔE (KJ/mol)
0	20	0.9512	8.94	1.097	−306.62
	40	1.0519	11.27	1.113	
	60	1.1187	13.14	1.124	
	80	1.1938	15.62	1.139	
5	20	0.6347	4.31	1.447	−414.81
	40	0.7633	5.80	1.448	
	60	0.8684	7.39	1.446	
	80	1.0122	10.29	1.458	

Figure 12   The plot of lg(Φ/T_p^2) versus $1/T_\mathrm{p}$ from the Kissinger method for PA6 and PAM/PA6 (5 wt %) composite.

$$\frac{d\left(\ln\dfrac{\Phi}{T_\mathrm{p}^2}\right)}{d\left(\dfrac{1}{T_\mathrm{p}}\right)} = -\frac{\Delta E}{R} \qquad (16)$$

where R is the gas constant and T_p is the peak temperature. Drawing a plot of $\ln\left(\Phi/T_\mathrm{p}^2\right)$ versus $1/T_\mathrm{p}$, we obtain a line with good linear relation in Figure 12; the slope = $d[\ln(\Phi/T_\mathrm{p}^2)]/d(1/T_\mathrm{p})$ = $-\Delta E/2.303R$, $\Delta E = -306.62$ and -414.81 KJ/mol for PA6 and PAM/PA6 composite. Therefore, the crystallization activity energy of PA6 matrix is clearly lowered by the addition of PAM rigid rod polymer.

CONCLUSION

Analyzing the crystallization half-time of isothermal and nonisothermal conditions, we can see that the PA6 overall crystallization rate of PAM/PA6 composite increases with the increasing of PAM content. The PAM rigid rod polymer functions as a nucleating agent to increase the crystallization rate of the PA6 matrix. This result is also supported by the analyses of the Avrami and Lauritzen–Hoffman equations. Mo's method fits the nonisothermal crystallization process very well for a broad range of cooling rates. Meanwhile, the activation energies are determined to be -306.62 and -414.81 KJ/mol for PA6 and PAM/PA6 (5 wt %) composite in the nonisothermal crystallization process from the Kissinger method. This result further shows the role of the heterogeneous nucleates of PAM in PA6 crystallization process.

References

1. Lenke, G. M. Composite polymeric materials; EP 0 408 166A2, 1991.
2. Campoy, I.; Gomez, M. A.; Marco, C. Polymer 1998, 39, 6279.
3. Takayanagi, M.; Ogata, T.; J Macromol Sci Phys 1980, B17, 591.
4. Li, Y.; Yu, J.; Guo, Z.;-X. J Appl Polym Sci 2002, 84, 827.
5. Morgan, P. W.; Pletcher, T. C.; Kwolek, S. J. Polym Prepr 1983, 24, 470.
6. Morgan, P. W.; Kwolek, S. J.; Pletcher, T. C. Macromolecules 1987, 20, 729.
7. Cheng, S. Z. D.; Janimak, J. J.; et al. Polymer 1989, 30, 494.
8. Zhang, S. Acta Polym Sinica 1989, 5, 552.
9. Bai, Z.; Jin, R.; Harris, F. W. Polym Prepr 1999, 40, 84.
10. Ding, H.; Ji, R.; Qu, X.; et al. China Plastics 2003, 17, 48.
11. Park, C.-S.; Lee, K.-J.; Nam, J.-D.; et al. J Appl Polym Sci 2000, 78, 576.
12. Tseng, C.-R.; Lee, H.-Y.; Chang, F.-C. J Polym Sci, Part B: Polym Phys 2001, 39, 2097.
13. Avrami, M. J Chem Phys 1941, 9, 177.
14. Avrami, M. J Chem Phys 1940, 8, 212.
15. Hoffman, J. D.; Weeks, J. J. J Chem Phys 1962, 37, 1723.
16. Liu, T.; Mo, Z.; Wang, S.; Zhang, H. Eur Polym Mater 1997, 33, 1405.
17. Turnbull, D.; Fisher, J. C. J Chem Phys 1949, 17, 71.
18. Hoffman, J. K.; Davis, G. T.; Lauritzen, J. I. In Treatise on Solid State Chemistry: Crystalline and Noncrystalline Solid; Hannay, N. B., Ed.; Plenum: New York, 1976; Vol. 3.
19. He, M.; Cheng, W.; Dong, X. Polymer Physics; Fudan University Press: Shanghai, 1993; p. 252.
20. Jeziorny, A. Polymer 1978, 19, 1142.
21. Ozawa, T. Polymer 1971, 12, 150.
22. Liu, T.; Mo, Z.; Zhang, H. J Appl Polym Sci 1998, 67, 815.
23. Liu, S.; Yu, Y.; Mo, Z. J Appl Polym Sci 1998, 70, 2371.
24. Kissinger, H. E. J Res Natl Stand 1956, 57, 217.